Pergamon

Phys. Chem. Earth (A), Vol. 24, No. 7, pp. 575–579, 1999

1464-1895/99/$ - see front matter

PII: S1464-1895(99)00082-4

Fracture Network Versus Single Fractures: Measurement of Fracture Geometry with X-ray Tomography

C. D. Montemagno[1] and L. J. Pyrak-Nolte[2]

[1]Department of Agriculture and Biological Engineering, Cornell University, NY 14853, U.S.A.
[2]Department of Physics, Department of Earth and Atmospheric Sciences, Purdue University, U.S.A.

Received 28 August 1998; accepted 15 December 1998

Abstract. Several long-standing questions concerning fluid transport in fractured rock involve the geometrical properties of the connected void space within a fracture network. We present experimental results that compare the geometrical properties of a fracture network to those of the individual fractures in the network. To image and quantify the aperture distribution of natural fracture networks in coal, a Wood's metal injection method is combined with X-ray computerized tomography and image analysis. We find that the aperture distribution of the networks is spatially anisotropic and dependent on the number and geometry of the individual fractures. Void area in the individual fractures ranged between 45% - 58%. A three-dimensional auto-correlation analysis on the fracture network and a two-dimensional analysis on the individual fractures found that the apertures were correlated over distances of 10 mm to 20 mm in the direction of flow.

1 Introduction

The flow of natural and industrial fluids in rock formations cannot be understood without a detailed knowledge of the statistical and topographical geometry of fracture networks. Fractures are the dominant flow paths in rock, and fracture networks provide the conduits that control production rates at gas and oil wells in fractured reservoirs and control the migration rates of biologically hazardous materials, including nuclear, chemical and biological waste (Sahimi, 1993). Numerical models for simulating fluid flow through a fracture network in three dimensions require data on the geometry of the network, such as spatial correlations, interconnectivity, fracture aperture, fracture length and orientation (Long et al., 1985 & 1991).

Typically, the geometry of real fracture networks are only measurable as two-dimensional planes or cross-sections, such as in rock outcrops, tunnel or excavation walls, or as thin sections after destruction of a rock sample. The difficulty in characterizing natural fracture networks in rock arises because three-dimensional networks are imbedded in a rock matrix that is opaque to almost all probes. Non-destructive imaging of three-dimensional fracture networks in natural rocks has been an elusive goal because rocks are opaque to most probes.

Confocal microscopy can be used for near-surface imaging or pore geometry in rock (Montoto et al., 1995; Fredrich et al., 1995), as well as traditional photomicroscopy (Gretsch, 1995). However, confocal microscopy techniques for near-surface imaging of pores and cracks fail for depths greater than several hundred microns, necessitating destructive sectioning of the originally intact rock, and is time consuming for areas exceeding 1 mm^2. In addition, imaging of fracture geometry under simulated in-situ conditions, i.e. under equivalent lithostatic stresses at depth, has only recently become practical (Cook et al., 1993). Advanced seismic techniques are currently being studied as a means of remote non-destructive detection of fractures (Pyrak-Nolte *et. al.*, 1990; Nihei et al, 1994). However, significantly more theoretical and technological development is needed to reconstruct the complex three-dimensional network geometry of natural fracture systems using seismic analysis.

This work presents an integrated fracture measurement and analysis system that has been developed to examine the relationship between fracture network geometry and the physical properties of the medium. In this report we use X-ray computerized tomography (CT) analysis and three-dimensional image analysis to investigate the three-dimensional geometry of fracture networks in bituminous coal cores. Application of this method has resulting in the development of a data set that presents a detailed description of the structural morphology of a three-dimensional fracture network under lithostatic conditions.

Correspondence to:
Carlo D. Montemagno
Cornell University
Agricultural and Biological Engineering Dept.
304 Riley-Robb Hall
Ithaca, NY 14853
Phone: (607) 255-2280
Fax: (607) 255-4080
E-mail: cdm11@cornell.edu

This characterization includes the statistical and spatial distribution of fracture apertures within a single connected network, including all connected apertures down to two microns and direct measurement of the variation in porosity of the connected fracture network as a function of distance along the core axis.

2 Experimental Set-up

In our study, we have analyzed the three-dimensional geometry of fracture networks and the geometry of several of the individual fractures within the network for two whole drill cores of bituminous coal. Core AA and BB were drilled from blocks of coal from the Sundance Formation in Pit #1 at the La Plata Coal Mine in the San Juan Basin, New Mexico. The dimensions of the cores are given in Table 1. Core AA was taken from the same block of coal as core BB but was drilled perpendicular to the bedding planes. Core BB was drilled parallel to the bedding planes and parallel to the dominant fracture set (face cleat).

Table 1. Data for Core AA and Core BB (from Pyrak-Nolte et al., 1997).

Sample Number	AA	BB
Length (mm)	44.1	112
Diameter (mm)	88.9	88.9
Bulk Volume (cm^3)	274	694
Confining Pressure at Solidification (MPa)	4.89	5.54
Nitrogen Pressure at Solidification (MPa)	0.49	0.44
Minimum Aperture Filled with Wood's Metal[1] (μm)	2.44 ± 1.2	2.74 ± 1.3
Weight of Injected Wood's Metal (g)	2.14	6.19
Volume of Connected Voids(cm^3)	0.22 ± 0.005	0.65 ± 0.013
Effective Cleat Porosity[2] (%)	0.082 ± 0.002	0.094 ± 0.002
Spacing between X-ray Scans (mm)	1.05	1.217
Constant of Proportionality, F ($\times 10^{-5}$)	7.11	5.03
Minimum Aperture from Image Analysis (μm)	2.22	2.62

[1] *Error from deviations in surface tension and contact angle of Wood's Metal* [2] *Error from deviations in the density of Wood's metal*

For this study, a combination of experimental techniques were used to quantify the aperture distribution of natural fracture networks in coal. The techniques used include (a) a Wood's metal injection method to form a cast of the connected void space and to quantify the volume of the connected void space within a fracture network; (b) computerized x-ray tomography to spatially locate the fracture to within 300 microns; and (c) medical imaging algorithms to resolve the apertures to within 2 microns. Below a brief summary of the experimental method is given. For more details, the reader is referred to Pyrak-Nolte (1991), Montemagno & Pyrak-Nolte (1995) and Pyrak-Nolte et al. (1997).

In the Wood's metal injection method, a low-melting-point metal is injected into coal cores subjected to reservoir stress conditions. A sample is placed in a hydrostatic pressure vessel and is subjected to the desired confining stress. The confining stress applied to Core AA and Core BB is given in Table 1. The injection system is heated to approximately 95 ^{0}C and the molten metal is injected in the coal core. After injection, the sample is cooled while the confining pressure and a nitrogen back pressure are maintained. When the metal has solidified, the sample is weighed to determine the weight of the metal injected. Using the gravimetric data and the density of the metal, the volume of voids injected is calculated. The smallest aperture penetrated by the metal is calculated using the surface tension of the metal, the pore pressure at solidification, and the Laplace equation for a cylindrical tube.

After the gravimetric analysis, the injected cores were scanned with a Philips Model Tomoscan 60/TX computerized x-ray tomographic system using 130 keV and a beam width of 2 mm. Because of beam hardening artifacts (Kak and Slaney, 1988), standard morphological transformations (Jain, 1989) were applied to the data to correct for the exaggerated thickness of the metal-filled fractures in the x-ray scans (Montemagno and Pyrak-Nolte, 1995). The morphological transformations resulted in single-pixel localization of the metal-filled fracture. The pixel size in each scan for each sample is 0.3 mm x 0.3 mm. For volumetric analysis, the voxel (three-dimensional pixel) volume was 0.3 mm x 0.3 mm x L_s, where L_s is the length between successive scans. The L_s for Core AA and Core BB are 1.05 mm and 1.217, respectively.

Pyrak-Nolte et al. (1997) extracted the aperture distribution for natural fracture networks in coal by relating the CT number of a specific voxel to the metal volume contained within that voxel (equation 1). The aperture within the n-th voxel is obtained by multiplying the CT_n number of that voxel by a factor F, which is constrained by the total volume of injected metal through the expression

$$F = t_{vox} \frac{V_{grav}}{V_{vox} \sum_{n=1}^{N} \left(CT_n - CT_{coal} \right)} \qquad (1)$$

where the sum is over all voxels and V_{vox} is the voxel volume, t_{vox} is the linear size of the voxel, V_{grav} is the total volume filled by injected metal, and CT_{coal} is the CT density associated with the coal matrix. The constant of proportionality F is given for each sample in Table 1. The

CT_{coal} for Core AA and Core BB are 1336 and 1448, respectively. These values differ from the CT values given in Pyrak-Nolte et al. (1995) because they were systematically chosen by examining the histogram of all CT numbers from the coal data and choosing the value were a change in slope occurred. This thresholding procedure of the images eliminates the non-fracture portions of the data, that is the coal matrix, shade fingers, bedding planes, etc.

Data on the geometry of a single fracture from a fracture network were obtained using customized computer software for selecting the fracture and tracking its location throughout the length of the core. This was performed by interactively selecting the region of interest on aperture images of the fracture network, i.e. images that contain the numerical value of the apertures for the fractures with the non-fracture portions of the image set to zero. Because the height of the selected region of interest was greater than one pixel (i.e. the spatial resolution), at each position the average of the apertures at a given position (over the height of the region of interest) was taken. This affects the size of the aperture at the intersections in the single fracture analysis. The size of the aperture at the intersections discussed in Pyrak-Nolte et al. (1997) was obtained by convolving the aperture image with a kernel containing information that locates the position of individual fracture intersections.

3 Results & Discussion

Figure 1 shows the geometry of the connected void space in four single fractures extracted from the fracture networks of Core AA and Core BB. Figure 1a&b contain the single fractures AA2 and AA4 taken from Core AA, while Figure 1c&d contains the single fractures BB1 and BB3 taken from Core BB. In Figure 1, red represented regions with large apertures (greater than 100 microns), and regions of green-purple represent regions with small apertures (~2 microns to 50 microns), and white regions represent regions with zero aperture (contact area). For fractures AA2 and AA4, the images represent a 60 mm by 42 mm region. For fractures BB1 and BB3, the images represent a 60 mm by 92 mm region. Fracture BB1 shown in Figure 1c was oriented orthogonal to the fracture BB3. The percent void space in fractures AA2, AA4, BB1, and BB3 is 58%, 53%, 45%, and 49%, respectively.

Pyrak-Nolte et al. (1997) compared the aperture distribution of the entire fracture network to the aperture distribution of the intersections. They found statistically that no significant difference in the aperture distributions of the intersections relative to the total network. They suggested that this discounts fracture intersections as dominant flow paths in terms of size but did not discount that the intersections may be preferentially connected across the core. The geometry of the flow paths in fracture BB1 shown in Figure 1c supports the hypothesis that fracture intersections may be preferentially connected. The long linear horizontal features in BB1 are the intersections between fracture BB1 and other orthogonal fractures. Some these orthogonal fractures (which are not shown) would not have connected flow paths if the fractures did not intersect. The void space geometry of the fractures in Core AA did not contain any clearly delineated intersections as those observed in Core BB. In fractures AA2, AA4, and BB3, the large void regions are connected by narrow channels. For understanding flow in single fractures, the geometry of these narrow channels support the concepts of either (a) a critical path (Pyrak-Nolte et al., 1988), that is, flow is strongly dominated by the path of highest aperture and in particular the point of smallest aperture along this path (critical neck); or (b) a preferential path (Yang, 1992), that is, flow is dominated by the path of least resistance. Further experimentation or numerical modeling is required to explore these concepts.

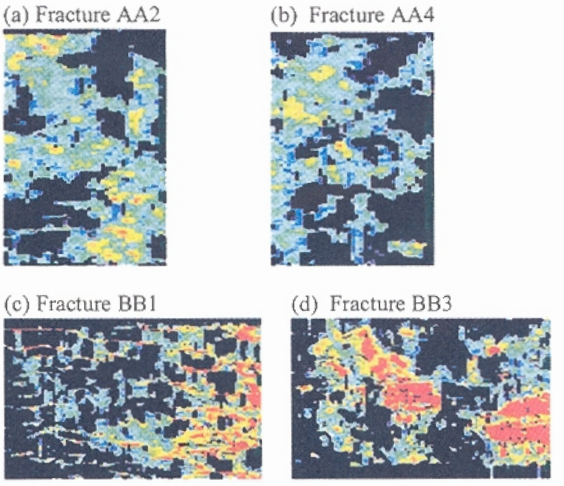

Fig.1. Extracted fractures from fractures networks in Core AA and Core BB. Red represents regions with large apertures (greater than 100 microns), and regions of green-purple represent regions with small apertures (~2 microns to 50 microns), and black regions represent regions with zero aperture (contact area). Fractures AA2 and AA4 are 42 mm by 60 mm. Fractures BB1 and BB3 are 92 mm by 60 mm. The arrow at the lower right hand corner of Fracture BB1 shows the approximate location of the intersection with fracture BB3.

Much of the recent experimental work on fractures has focused on understanding the relationship between fluid flow and fracture aperture and has used imaging to quantify the aperture distributions observed in single fractures. Figures 2 and 3 show the aperture distribution for the entire fracture network for Core AA and Core BB, and the aperture distribution for the single fractures shown in Figure 1. The aperture distribution for Core AA and fractures AA2, AA4, and BB3 were fit well with a gaussian distribution, while Core BB and fracture BB1 were better fit with a lognormal distribution. Other researchers have measured fracture apertures using surface topography (Durham & Bonner, 1995; Durham, 1997; Iwano & Einstein, 1995), void casting or injection (Gale, 1987; Gentier et al., 1989; Hakami, 1990 & 1995) and x-ray tomography (Pyrak-Nolte et al., 1997; Keller, 1997). For a wide variety of fracture samples, these researchers found that the aperture size distribution for single fractures can be either gaussian or log-normal.

In the field or in the laboratory, measurements of fracture network geometry are traditionally made in two-dimensions to determine the important features of the fracture networks such as fracture orientation, spacing, aperture visible at the surface of the rock, porosity, or single fracture geometry. The two-dimensional data-sets are used to reconstruct the three-dimensional fracture network. However, extrapolating two-dimensional datasets to three-dimensions assumes a certain spatial correlation among the fractures. Pyrak-Nolte et al. (1997) examined the spatial correlation among the apertures by performing a three-dimensional auto-correlation analysis on the three-dimensional fracture network. They found that the apertures in core AA and BB were correlated over distances of 6 mm to 30 mm and the correlation slope differed between the two-orthogonal directions (-0.92 vs -1.25). They hypothesized that the difference in the correlation exponent for the two orthogonal directions suggested that the aperture network structure in cores AA and BB, were self-affine structure.

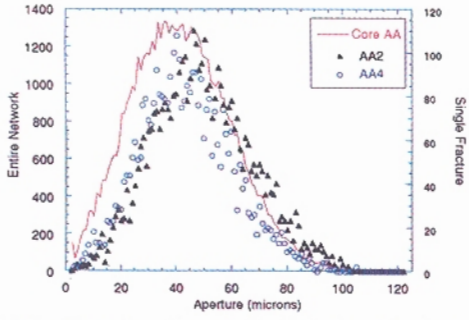

Fig.2. Comparison of aperture distribution for entire fracture network in Core AA (solid line) with the aperture distributions of two fractures, AA2 (triangles) and AA4 (circles), extracted from the network.

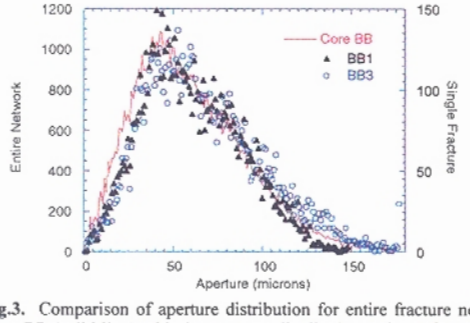

Fig.3. Comparison of aperture distribution for entire fracture network in Core BB (solid line) with the aperture distributions of two fractures, BB1 (triangles) and BB3 (circles), extracted from the network.

In this paper, we performed a two-dimensional auto-correlation analysis on fractures AA2, AA4, BB1, and BB3 to compare (Figure 4 & 5) with the results of three-dimensional auto-correlation analysis performed on Core AA and Core BB by Pyrak-Nolte et al (1997). The auto-correlation functions shown were taken in the direction parallel to the metal injection, i.e., along the length of the core (Core AA ~ 42 mm; Core BB ~ 92 mm). For both fracture networks and the single fractures, the apertures were correlated over distances (correlation lengths) of 15 mm to 20 mm. To compare the correlation slopes from the three-dimensional and two-dimensional auto correlation analysis, we use D-E=S, i.e., the fractal dimension, D, minus the Euclidean dimension, E, of the analysis is equal to the correlation slope, S. From this relationship, the fractal dimension of the spatial distribution of the apertures in the direction parallel to the metal injection is ~1.7 for both the fracture network and the single fractures. Below the correlation length, the scaling function of the spatial distribution of the apertures depends on the fractal dimension. Above the correlation length, spatial distribution of the apertures depends on the Euclidean dimension and is considered homogeneous. This suggests that measurements on the core scale can be scaled to the field scale once a sample is larger than the correlation length.

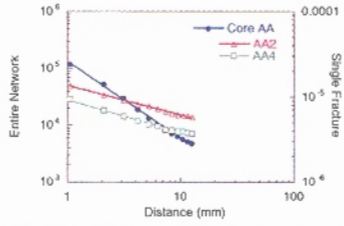

Fig.4. Comparison of autocorrelation functions for entire fracture network in Core AA (circles) with the autocorrelation functions of two fractures, AA2 (triangles) and AA4 (squares), extracted from the network. The analysis is taken in direction of the metal injection. The autocorrelation functions for Core AA and fractures AA2 and AA4 have slopes of −1.3 and −.35, respectively.

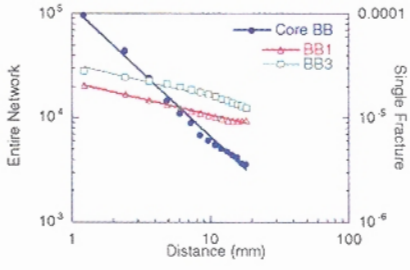

Fig.5. Comparison of autocorrelation functions for entire fracture network in Core BB (circles) with the autocorrelation functions of two fractures, BB1 (triangles) and BB3 (squares), extracted from the network. The analysis is taken in direction of the metal injection. The autocorrelation functions for Core BB and fractures BB1 and BB3 have slopes of −1.2 and −0.31, respectively.

4 Summary

We have presented a methodology to microscopically describe the three-dimensional structure of fracture networks in rocks. Using the Wood's metal injection method in conjunction with x-ray tomographic imaging and three-dimensional image analysis, it is now possible to investigate the detailed structure of fracture networks under lithostatic conditions. The tomographic imaging of high-density and high-contrast metal injected into the fracture network is combined with accurate gravimetric measurements to yield a determination of the fracture apertures with an uncertainty of only one micron. This high accuracy is achieved despite a smaller accuracy for the spatial location of the fracture apertures of only 300 microns. Applying this technique to single cores of bituminous coal, we not only obtained quantitative values for the sizes and spatial distributions of the fracture apertures but also a map of fracture connectivity. The unique and accurate data set that is provided by this technique should be valuable input for understanding the scaling behavior of fracture networks and should provide direct answers for a broad range of related flow and transport problems.

Acknowledgments. CDM and LJPN wishes to acknowledge the Gas Research Institute Contract Number 5092-260-2507, Amoco Production Research, the National Science Foundation - Young Investigator Award from the Division of Earth Sciences (NSF-9896057), and the Department of Energy, EMSP program for support of this research.

References

Cook, J.M., Goldsmith, G., and Auzerais, F., 1993. X-ray tomography studies of wellbore processes under in situ stress conditions. *Int. J. Rock Mech., 30:7*:1091-1094.

Durham, W.B., 1997. Laboratory observations of the hydraulic behavior of a permeable fracture from 3800 m depth in the KTB pilot hole. *J. Geophys. Res. 102:B9*:18405-18416.

Durham, W.B. and Bonner, B.P., 1995. Closure and fluid flow in discrete fractures. In L.R. Myer, N.G.W. Cook, R.E. Goodman & C.F. Tsang (eds) *Fractured and Jointed Rock Masses. 441*:446. Rotterdam: Balkema.

Fredrich, J.T., Menendez, B., and, Wong, T. F, 1995. Imaging the pore structure of geomaterials. *Science, 268*:2776:2779.

Gale, J.E. 1987. Comparison of coupled fracture deformation and fluid models with direct measurements of fracture pore structure and stress-flow properties. In I.W. Farmer, J.J.K. Daemen, C.S. Desai, C.E. Glass & S.P. Neuman. (eds) *Rock Mechanics*: Proceedings of the 28th US Symposium, Tucson, Arizona. Rotterdam. 1213-1222. Rotterdam: Balkema.

Gentier, S., Billaux, D., and Vliet, L. van., 1989. Laboratory testing of the voids in a fracture. *Rock Mechanics and Rock Engineering. 22*:149-157.

Gertsch, L.S., 1995. Three-dimensional fracture network models from laboratory-scale rock samples. *Int. J. Rock Mech. Min. Sci. & Geomech. Abstr., 32:1*:85-91.

Hakami, E., 1988. Water flow in single rock joints. Licentiate. Thesis. Lulea University of Technology. Sweden.

Hakami, E., 1995. Joint aperture measurements - An experimental technique. In L.R. Myer, N.G.W. Cook, R.E. Goodman & C.F. Tsang (eds) *Fractured and Jointed Rock Masses. 453*:456. Rotterdam: Balkema.

Iwano, M. and Einstein, H. H.. 1995. Laboratory experiments on geometric and hydromechanical characteristics of three different fractures in granodiorite. In T. Fujui (ed.) *Proceedings of the Eight International Congress on Rock Mechanics. 2*:743;750. Rotterdam: Balkema.

Jain, A.K., Fundamentals of Digital Image Processing, Prentice Hall, New Jersey, 1989.

Kak, A.C. and Slaney, M., Principles of Computerized Tomographic Imaging, IEEE Press, New York, 1988.

Keller, A.A. 1997. High resolution cat imaging of fractures in consolidated materials. In K. Kim (ed.) *Proceedings for the 36th U.S. Rock Mechanics Symposium and ISRM International Symposium. 1*:97:106. New York: Columbia University.

Long, J.C.S. and Witherspoon P.A., 1985. The relationship of the degree of interconnectivity to permeability in fracture networks. *JGR, 90*:3087-3098.

Long, J.C.S., Karasaki, K., Davey, A., Peterson, J., Landsefeld, M., Kemeney, J., and Martel, S., 1991. Inverse approach to the construction of fracture hydrology models conditioned on geophysical data. An example from the validation exercises at Stripa mine, International Journal of Rock Mechanics, *Mining Sciences & Geomechanics Abstracts, 28*:2-3:121-149.

Montoto, M., Martinez-Nistal, A., Rodriguez-Rey, A., Fernandez-Merayo, N., and Soriano, P., 1995. Microfractography of granitic rocks under confocal scanning laser microscopy, *J. Microscopy. 177:2*:138-149.

Montemagno, C.D. and Pyrak-Nolte, L.J., 1995. Porosity of natural fracture networks, *Geophys. Res. Lett., 22:11*:1397-1400.

Nihei, K.T., Myer, L.R., Cook, N.G.W., and Yi, W., 1994. Effects of non-welded interfaces on guided SH-wave, *Geophysical Research Letters, 21:9*:745-748.

Pyrak-Nolte, L.J., Cook, N.G.W., and. Nolte, D.D, 1988. Fluid Percolation through Single Fractures, *Geophysical Research Letters, 15:11*:1247-1250.

Pyrak-Nolte, L.J., Myer, L.R., and Cook, N.G.W., 1990. Transmission of seismic waves across natural fractures, *Journal of Geophysical Research, 95:B*:8617-8638.

Pyrak-Nolte, L.J., The Feasibility of Using Wood's Metal Porosimetry Techniques to Measure the Fracture Void Geometry of Cleats in Coal, Topical Report, Gas Research Institute, *GRI-91/0373*, pp22 (Dec. 1991).

Pyrak-Nolte, L.J., Yang, G., Montemagno, C.D., Myer, L., and Cook, N.G.W, 1995. Three-dimensional tomographic visualization of natural fractures and graph theory analysis of the transport properties, Proceedings of 8th International Congress on Rock Mechanics, eds. T. Fujii, Tokyo, Japan, Sept 25-29, 1995, Pubs. A. A. Balkema, Rotterdam, 2:855-859.

Pyrak-Nolte, L.J., Montemagno, C.D. and Nolte, D. D, 1997. Volumetric imaging of aperture distributions in connected fracture networks, *Geophysical Research Letters, 24:18*:2343-2346.

Sahimi, 1993. Flow phenomena in rocks: from continuum models to fractals, percolation, cellular automata, and simulated annealing, Rev. *Mod. Phys., 65*:1393-1534.

Yang, G., 1992. Computer Aided Analysis of Groundwater and Polluntant Migration caused by Strata Movement, Ph.D. Thesis, University of California.